THERMAL ANALYSIS AND OPTIMIZATION OF *L*-SHAPE FIN HEAT SINK UNDER NATURAL CONVECTION USING ANOVA AND TAGUCHI

by

Numan HABIB[a]***, Muftooh Ur Rehman SIDDIQI***[a*]***, and Muhammad TAHIR***[b]

[a] Mechanical, Biomedical, and Design Engineering Department,
School of Engineering and Technology, Aston University, Birmingham, UK
[b] Department of Mechanical Engineering, Bahauddin Zakriya University,
Multan, Pakistan

Original scientific paper
https://doi.org/10.2298/TSCI210612317H

Advancement in electronic systems resulted in miniaturization and high-power densities. Therefore, the rate of heat generation in circuit board increased dramatically. To overcome the problem of overheating, numerous heat sink designs are proposed including L-shape fins heat sink. The thermo-fluidic flow behavior and temperature difference are analyzed to get better understanding of heat transfer from the sink to ambient air. Governing equations for the model of conjugate heat transfer in 3-D environment are solved and discretized across the computational domain. Numerous experiments are carried out to validate the numerical results. The effect of fin numbers, height, and heat sink size at three different input power is reported. Furthermore, ANOVA and Taguchi statistical methods are used to predict parameters that affect the heat transfer. The study revealed that fin height affects the heat transfer rate the most, and accounts for 25.3% increase in heat transfer rate. Optimization of the heat sink is carried out to ensure better efficiency of the proposed heat sink. The optimized conditions for the sink are observed to be heat sink size of 90 mm, 9 number of fins, and 33 mm of fin height.

Key words: *L-shape heat sink, thermal management, thermal analysis, novel heat sink design*

Introduction

Due to compact structural design of the modern electronic devices, unwanted heat is produced in the circuit boards. High thermal densities decrease the life of the electronic chip, hence, proper thermal management is needed to extract unwanted heat from the system. Heat sinks made of aluminium alloy are commonly used cooling systems (active and passive) to extract heat from the system and dump into the environment. Heat transfer depends on the material properties and contact area between two materials. Many fins are mounted vertically on the horizontal base plate to maximize the area of contact. Currently, conventional heat sink with straight fins is commonly used due to the simple geometry, low cost of manufacturing

* Corresponding author, e-mail: m.siddiqi5@aston.ac.uk

and high heat transfer rate. Research have been carried out recently on straight fin heat sink to study thermos-fluidic flow and optimize different input parameters.

Huang and Tung [1] studied the performance of wavy shape heat sink both experimentally and numerically. Further, Duan *et al.* [2] analyzed pressure drops and fluid--flow characteristics in heat sink with plate fins and bottom profile of elliptic shape. Alfellag *et al.* [3] used conjugate model of heat transfer and numerically studied the thermo-fluidic flow in mini channel heat sink with triangular shape fins. They claimed Nusselt number improved by 1.5 at angle of 55° for the full height slot. Further, they observed that hydrothermal factor of performance enhanced by 1.43. Abdelmohimen *et al.* [4] studied the effect of rod on heat transfer with various configurations in plate fin heat sink. They claimed that for the studied range of Reynolds number optimal case of heat transfer was achieved when four rods are placed through fins. Wiriyasart and Naphon [5] targeted liquid on different shapes of fin *i.e.* circular, rectangular, and conical to enhance heat transfer. However, results revealed a very small improvement in thermal resistance. Freegah *et al.* [6] proposed fillet profile in plate fin heat sink and numerically investigated improvement in heat transfer rate. Numerous studies are carried out to investigate and improve heat transfer in heat sink by using PCM [7-10]. Nair [11] proposed a method to enhance heat transfer through convection of plate fin heat sink by introducing additional shrouds to the top and bottom of the sink.

Conventional heat sink was studied by Jones and Smith [12]. They found inter fin distance and fin height are important parameters and affect the heat transfer rate drastically. Bar-Cohen [13] concluded that optimal fin thickness varies with combination of different parameters, *i.e.*, material, environmental, and geometric constrains. Teertstra *et al.* [14] carried out experimentations and presented analytical model for pin fin heat sink under natural convection. They revealed that the presented analytical model could be used calculate heat transfer rate to choose suitable heat sink according to the specific specification. Baskaya *et al.* [15] carried numerical studies and investigated various input parameters, included inter-fin distance, heat transfer rate and temperature deference. They observed that increasing the fin height results in high heat transfer rate. Furthermore, de Lieto Vollaro *et al.* [16] numerically studied straight fin heat sink in vertical orientation. They focused on thermal conductivity, emissivity, dimensions of heat sink and other working fluid properties. Tari *et al.* [17] studied different combinations of input parameter in straight fin heat sink including fin length, fin height, heat sink orientation and spacing between the fins, under natural convection and suggested correlations.

Shen *et al.* [18] experimentally and numerically investigated the effect conventional heat sink orientation on heat transfer rate. They suggested correlations for different orientations and Reyleigh numbers. Naik *et al.* [19] considered the fact that heat sinks are usually placed in enclosed electronic system and placed a straight fin heat sink under an adiabatic shroud. They experimentally investigated the heat transfer rate under natural convection. They concluded that the heat transfer rate is directly proportional to the clearance between the heat sink and shroud.

To enhance heat transfer rate both in active and passive convection various designs are proposed and studied *i.e.*, straight fins with slope [20], straight fins with perforations [21], straight fins with square and circular cross-sections [22], straight fins with circular arrangement [23], and straight metal foam fins [24]. Furthermore, Kim [22] studied heat transfer rate with various cross-section designs mounted vertically on base plate under natural convection. Ledezma and Bejan [20] improved heat transfer performance of the conventional heat sink by introducing slope to the fins. Furthermore, Jang *et al.* [23] experimentally studied radial heat sink and optimized its design in terms of thermal resistance. Costa and Lopes [24] introduced technique to obtain specific cooling with minimum material and mass usage. Jang *et al.* [25] and Li *et al.* [26] found that the heat transfer rate is improved for the radial heat sink by introducing a chimney. In addition, Elshafei [21] proposed hollow straight fins and claimed that improved heat transfer performance was achieved.

In a recent study, Chamkha *et al.* [27] investigated various parameters such as Rayleigh number, heat generation and volume fraction for slant porous cavity and nanoparticles. The author claimed that, addition of nanoparticles for several Rayleigh numbers reduced the heat transfer rate. Furthermore, Kargarsharifabad [28] numerically and experimentally investigated heat transfer rate for Cu-water nano-fluid under natural convection. The author concluded that, heat transfer is decreased when the volume fraction of nanoparticles is increased. In another study [29] the same author used genetic algorithm and numerical simulations and optimized the arrangement of both obstacles and conducting fins. An increase of 1.63 times in heat transfer for obstacles fins was noted when compared to conducting fins. Recently, Chamkha *et al.* [30] studies gamma-shaped porous cavity with Cu-water nanofluid and in the presence of magnetism. The study revealed that increase in nanoparticles volume fraction affect the entropy production more than enhancement in heat transfer rate. Bahmani and Kargsharitabed [31] investigated horizontal flat plate heat exchangers under natural convection and constant heat flux. The results revealed that for Prandtl number higher than 1, low Nusselt number was achieved. However, the reverse trend was observed for Prandtl number less than 1 and another study [32] a correlation was derived from numerical simulation results.

The *L*-shape heat sink design is proposed in previous studies to enhance heat transfer rate. However, no study has been carried out on its optimization. In the present study, experiments and simulations are carried out to better understand fluid flow and heat transfer mechanism in *L*-shaped heat sink under natural convection. Furthermore, ANOVA and Taguchi methods are used to optimize the heat sink and analyze the effect of input parameters on the heat transfer rate. In addition, the effect of clearance between heat sink and shroud is also investigated by keeping the fact in mind that heat sink are usually kept in enclosures. A numerical model was validated through experimentations under natural convection.

Materials and methods

Governing equations

Following assumptions are made with computational model:

- The air-flow is incompressible, laminar, and steady.
- The fluid used in the model is considered to be Newtonian.
- Only heat transfer through conduction and convection is considered. However, heat transfer through radiation is neglected.
- Body forces and viscous dissipation effects are neglected.

Based on the assumptions, the energy, momentum and continuity equations in the three dimensions are [33]:

Equation of energy:

$$\left[\frac{\partial T}{\partial x}(u)+\frac{\partial T}{\partial y}(v)+\frac{\partial T}{\partial z}(w)\right]C_p\rho=\left[\frac{\partial^2 T}{\partial x^2}(u)+\frac{\partial^2 T}{\partial y^2}(u)+\frac{\partial^2 T}{\partial z^2}(w)\right]k \quad (1)$$

Equations of momentum:

$$\left[\frac{\partial u}{\partial x}(u)+\frac{\partial u}{\partial y}(v)+\frac{\partial u}{\partial z}(w)\right]\rho=\mu u\nabla^2-\frac{\partial_p}{\partial x} \tag{2}$$

$$\frac{\partial v}{\partial x}u+\frac{\partial v}{\partial z}w+\frac{\partial v}{\partial y}v=\nabla^2 uv+(T-T_\infty)\beta \mathrm{g} \tag{3}$$

$$\left(\frac{\partial w}{\partial x}u+\frac{\partial w}{\partial z}w+\frac{\partial w}{\partial y}v\right)\rho=\mu w\nabla^2-\frac{\partial_p}{\partial x} \tag{4}$$

Equations of continuity:

$$\frac{\partial u}{\partial x}+\frac{\partial w}{\partial z}+\frac{\partial v}{\partial y}=0 \tag{5}$$

where u, v, and w, x, y, and z, are directions, C_p – the heat capacity, ρ – the density of fluid, β – the coefficient of thermal of expansion, T – the heat sink surface temperature, k – the thermal conductivity of material, and T_∞ – temperature of ambient air is specified with. However, heat loss due to radiation is not considered [34].

Equation for the coefficient of heat transfer for convection is given [35]:

$$h_{\mathrm{avg}}=\frac{Q}{(T_{\mathrm{sur}}-T_{\mathrm{air}})A} \tag{6}$$

For the power input following equation is used:

$$P_{\mathrm{in}}=VI \tag{7}$$

where V is voltage and I is current.

Equation for thermal resistance in convection:

$$R_{\mathrm{Con}}=\frac{1}{hA} \tag{8}$$

In the eqs. (6) and (7), A is surface area and h is the heat transfer coefficient for convection.

Gauge pressure at inlet (x = 0) is applied, inlet gauge pressure with uniform distribution was applied:

$$T_{\mathrm{f}}=T_{\mathrm{in}} \tag{9}$$

$$p=p_{\mathrm{in}} \tag{10}$$

At the heater power of constant value is applied at y = 0.

$$-k_s\frac{\partial T_{\mathrm{s}}}{\partial y}=q \tag{11}$$

Adiabatic boundary condition is applied to the remaining surfaces:

$$\frac{\partial T_s}{\partial z} = \frac{\partial T_s}{\partial y} \tag{12}$$

Computational domain set-up

The *L*-shape fins heat sink with variation in fin number, fin height and heat sink sizes are considered in the current study. As shown in fig. 1, a computational model of length 1200 mm, and width and length of 120 mm is taken. Surface at $X = 0$ mm is taken as inlet and surface at $X = 1200$ mm is taken as outlet. In addition, remaining surfaces are considered to be adiabatic walls. The studied heat sink, *L*-shape finned heat sink with various configuration is placed at the center of the computational domain as shown in fig. 2. A constant fin thickness of 2 mm is considered with variation in fins height of 10 mm, 20 mm and 30 mm. Table 1 shows the properties of materials used in the current study. A constant ambient temperature of 300 K is considered with three different input powers *i.e.*, 20 W, 40 W, and 60 W.

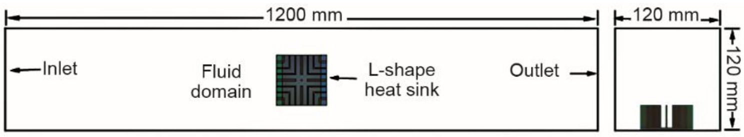

Figure 1. Computation domain

Figure 2. Model of conventional heat sink

Table 1. The heat sink and ambient air properties [33]

Property	Unit	Ambient air	Heat sink
C_p	[$\mathrm{Jkg^{-1}K^{-1}}$]	1000	870
K	[$\mathrm{Wm^{-1}K^{-}}$	0.0242	200
P	[$\mathrm{kgm^{-3}}$]	1.225	2700

Grid independency and solution method

In the current study, CFD commercial code of IcePack (ANSYS®) version 15.0 is used to carry out 3-D simulations numerically. Upwind scheme of 2nd order is considered for the convective terms. However, 2nd order difference scheme is considered for diffusion terms. Furthermore, SIMPLE algorithm is used for the pressure and velocity coupling. For momentum and continuity, a convergence criterion was set to less than 10^{-6}. Core i5 computer with RAM of 8 GB and processors of 2.5 GHz was used to conduct simulations.

It was ensured through mesh independency test that the generated solution is independent of mesh size. Element numbers varied from 325344 to 1119136 for the constant input power of 20 W. For any N, relative percent error, $e\%$, was calculated using eq. (13) between the course and finer mesh (N_1 and N_2):

$$e\%_N = 100\frac{N_2 - N_1}{N} \tag{13}$$

As illustrated in tab. 2, relative error, $e\%$, less than 0.5% is observed in element number at 0.8 million based on ΔT value. In the current study, Mesh number 3 is considered and is adequate to get acceptable results.

Table 2. Mesh independency test

Mesh number	Grid numbers	Temperature difference	*e*%
1	325344	54.79	3.59
2	519917	51.49	1.49
3	822371	50.09	0.48
4	919922	49.89	0.19
5	1118225	49.79	–

Experimental set-up

In the present study, free and forced convection apparatus, model TH320, manufactured by ESSOM (Thailand) was used to record experimental results. Different temperature sensors were mounted on various positions to record temperature *i.e.*, inlet, outlet, ambient air and heat sink temperatures. Furthermore, voltmeter and ammeter were used to measure input power to the heater.

As shown in fig. 3, heat sink was mounted on heater in free and forced convection apparatus using thermal paste to ensure maximum heat transfer from heater to the sink without heat loss. An insulation made of rock wood was placed on the bottom surface of the heater to prevent heat loss. Thermal sensors (*K*-type thermocouples) at five different positions were mounted to record temperatures. Furthermore, two sensors were placed at inlet and outlet of the channel. All thermocouples were connected to TC-08 for data acquisition and the data was stored in a computer connected to the acquisition system. The heat power was displayed by ammeter and voltmeter connected to the heater, and varied through a knob in control box.

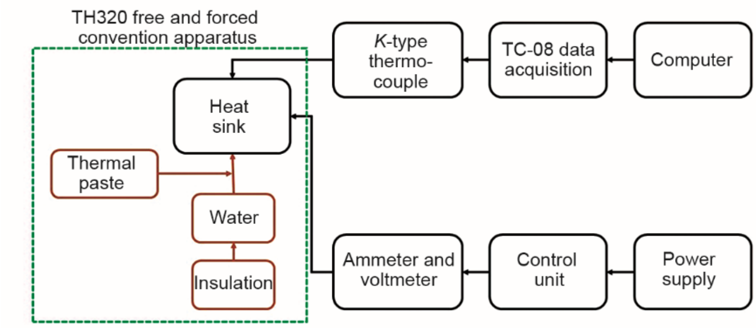

Figure 3. Experimental set-up schematic

Experimentation in the current study was carried out in a laboratory with a room temperature and without HVAC system. Control unit was used to feed accurate input power of 20 W, 40 W, and 60 W. Ammeter and voltmeter were used to monitor voltage and current and calculate the input power to the heater. Data of all the thermocouples was recorded in the condition of steady state which was set to 0.5 ^{o}C temperature change per hour. Accurate data was ensured by repeating each experiment three times.

Aluminium alloy 6063 was used to manufacture *L*-shape fins heat sink. The alloy has thermal conductivity of 200 W/mK. A 100 mm by 100 mm single heater was used. The sink was manufactured with 9 fins and fin height of 20 mm. However, the base of the sink was taken 3 mm.

Equations (14) and (15) is used to calculate measurement uncertainties in the experimental set-up [36]. According to the provided manual from the manufacturer, current and voltage reading accuracy is 0.1%. Using the concept of the uncertainty in [37]. Furthermore, the effect of radiation is neglected; therefore, the heat supplied to the system is assumed to be equal to heat transfer rate [38]:

$$\frac{\Delta q_{\text{in}}}{q_{\text{in}}} = \frac{\Delta P_{\text{in}}}{P_{\text{in}}} = \sqrt{\left(\frac{\Delta I}{I}\right)^2 + \left(\frac{\Delta V}{V}\right)^2} \tag{14}$$

$$\frac{\Delta q_{\text{in}}}{q_{\text{in}}} = \frac{\Delta R}{R} = \sqrt{\left[\frac{\Delta(\Delta T)}{T}\right]^2 + \left[\frac{(\Delta q)}{q}\right]^2} \tag{15}$$

Maximum uncertainty in the heat transfer rate is calculated to be 6% by putting both the V and I values in eq. (14). However, the maximum error in thermocouples is given 0.1 K by the manufacturer. Using this information error in temperature measurement, ΔT, can be calculated. Average experimental uncertainties is calculated to be 3.5% for the thermal resistance.

Results and discussion

Model validation

To validate numerical model, experimentation has been carried out. The experimental and numerical results on the bases of temperature difference for *L*-shape fins heat sink are plotted as shown in fig. 4. Between experimental and numerical results, a slight difference of less than 9% is observed. The difference could be due to the error in sensors and input power to the heater. Furthermore, the difference could be due to heat loss to environment during experimentation, while in numerical solution all four walls were taken insulated. Overall, the numerical results show good agreement with numerical result. Hence, the model could be used for thermal analysis.

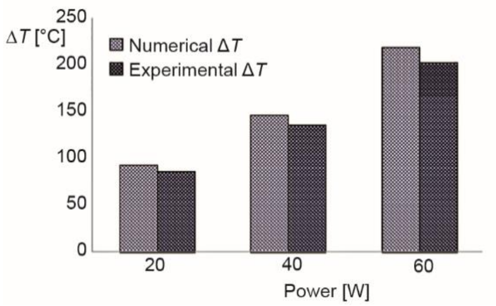

Figure 4. Experimental *vs.* numerical results for *L*-shape heat sink

Effect of input parameters

Effectiveness of heat sink is dependent on the temperature difference between heat sink and surrounding. With various combination of input variables experimentation and simulations were carried out and temperature differences were recorded. As shown in fig. 5, the temperature difference increases as input power increases. At maximum input power high thermal energy is generated inside the chip and maximum heat is transferred to the heat sink which results in high difference in temperature.

A declination is observed in temperature difference when number of fins are increased from 5-9 as shown in fig. 6. The increase noted is due to the increase in the contact area between heat sink and surrounding air which results in high heat transfer. Furthermore, steep declination of temperature difference can be seen when number of fins are increased from 5-7. However, further increase in fins from 7-9, the steepness reduces as the inter pin distance reduces, which results in drop in velocity and increase in fraction between the channel surface and air. Furthermore, the performance of *L*-shape heat sink increases when the number of fins increases. This is due to the fact that more number of fins offers more area for heat transfer and maximum heat is exchanged between the air and heat sink.

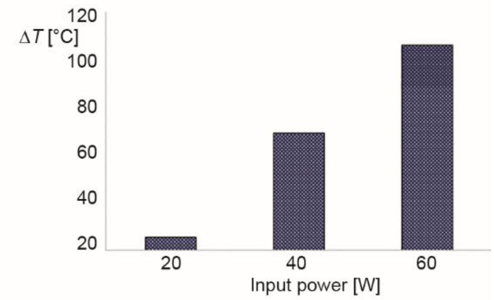

Figure 5. The ΔT *vs*. input power

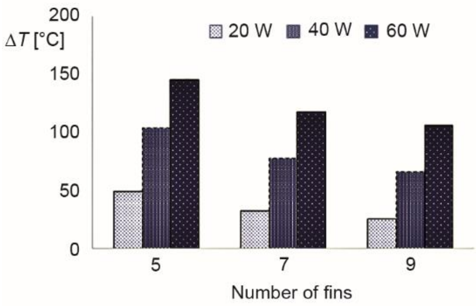

Figure 6. The ΔT *vs.* fins number

As shown in fig. 7, the temperature difference increases when the fins height increases. This is due to the fact that heat transfer is directly proportional the contact area. As the fin height increase extra material added which provides more area for heat to transfer to surrounding air through convection. With increase in fin height from 10-30 mm the heat dissipation mechanism improves and temperature deference drops. At high input power, little difference in temperature difference is noted.

The *L*-shape fins heat sink depicts similar gradual decreasing behaviour when the size of heat sink increases from 50-90 mm as shown in fig. 8. Furthermore, heat sink size offers extra material addition like number of fin and fin height, which results in increase in surface area of the sink and leads to high heat transfer rate.

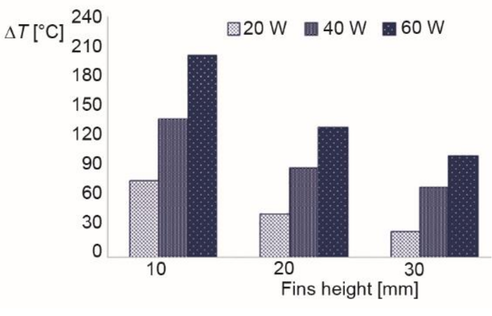

Figure 7. The ΔT *vs*. fins height

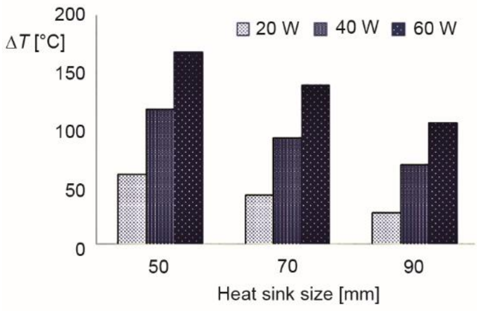

Figure 8. The ΔT *vs*. heat sink size

Effect of enclosure

The heat sink are usually placed in enclosures as shown in fig. 1. In this study, simulations were carried out to understand the effect of shroud on heat transfer. As shown in fig. 9, the temperature at side A is slightly higher when compared to side B. At side A maximum temperature of 53.15 °C is recorded. However, at side B the recorded temperature is 52.90 °C. The difference in both sides is due to the fact that clearance between side A and shroud is minimum which prevent fresh air circulation. Hence, results in low heat transfer. However, the clearance between shroud and side B is maximum which allow large amount of fresh air to come in contact with heat sink and result in high heat transfer.

Clearance between heat sink and top wall of the shroud is also considered in the present study and illustrated in fig. 10. Three cross-sectional planes show the temperature distribution in fluid domain at 10 mm, 20 mm, and 30 mm height. At 10 mm plane a small stagnation zone is formed, while the stagnation zone increases when the height increases. This is due to the top wall of the shroud which prevents the air to flow and result in large stagnation area.

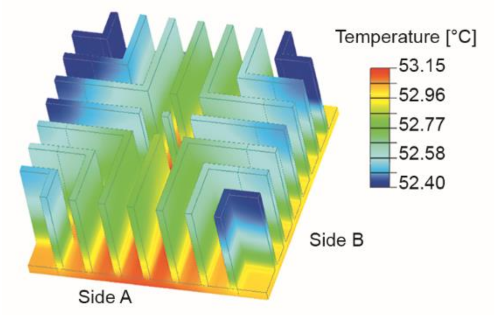

Figure 9. Temperature distribution on heat sink under shroud

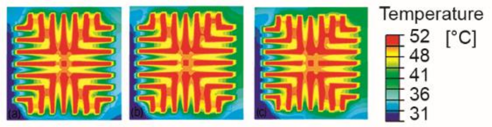

Figure 10. Temperature distribution in fluid domain at (a) 10 mm, (b) 20 mm, and (c) 30 mm

Taguchi

Signals to noise ratios are shown in tab. 3 with input factors and their levels. Factors are ranked on the basis of their effect on average temperature. Smaller is the better model was used to rank input parameters according to their contribution. Power factor is ranked first which depicts that power has more influence on average temperature and accounts for 46.8%. In addition, fin height is the second most important factor and its contribution is 25.3%. While, heat sink size and number of fins are ranked third and fourth, respectively and have no significant effect. Collective effect of heat sink size and fin numbers accounts for 27.9%.

Table 3. Response table for signal-to-noise ratios

Level	Heat sink size [mm]	Power [W]	Number of fins	Fin height [mm]
1	–44.43	–38.84	–44.06	–45.39
2	–43.41	–43.72	–42.90	–42.79
3	–41.45	–46.74	–42.33	–41.12
Delta	2.98	7.90	1.73	4.27
Rank	3	1	4	2

The ANOVA

Experimental results at a confidence level of 95% is evaluated using ANOVA. Analyzing P-values in the analysis of variance shown in tab. 4, all the parameters have significant effect on the output result. Combination of heat sink size and no of fins, heat sink size and power and heat sink size and fin height have also significant influence on temperature difference. However, other combination of the input factors on temperature difference is found to be insignificant. Further, observing F-value in ANOVA and signal-to-noise ratio in Taguchi, it is noted that power and fin height have great influence on temperature difference. In two factor combination, model F-value for power and fin height is maximum, which significantly affect the results when compare to other combinations.

Table 4. Analysis of variances

Source	DF	Adj SS	Adj MS	F-Value	P-Value	Status
Heat sink size	2	32098	16049	465.28	0.000	Significant
Power	2	238081	119041	3451.19	0.000	Significant
Number of fins	2	12129	6065	175.82	0.000	Significant
Fin height	2	76812	38406	1113.45	0.000	Significant
Heat sink size × power	4	2379	595	17.24	0.000	Significant
Heat sink size × number of fins	4	326	82	2.36	0.097	Insignificant
Heat sink size × fin height	4	401	100	2.91	0.055	Insignificant
Power × number of fins	4	1853	463	13.43	0.000	Significant
Power × fin height	4	6849	1712	49.64	0.000	Significant
Number of fins × fin height	4	181	45	1.31	0.309	Insignificant
Heat sink size × power × number of fins	8	383	48	1.39	0.274	Insignificant
Heat sink size × power × fin height	8	615	77	2.23	0.082	Insignificant
Heat sink size × number of fins × fin height	8	265	33	0.96	0.498	Insignificant
Power × number of fins × fin height	8	400	50	1.45	0.250	Insignificant
Error	16	552	34			
Total	80	373324				

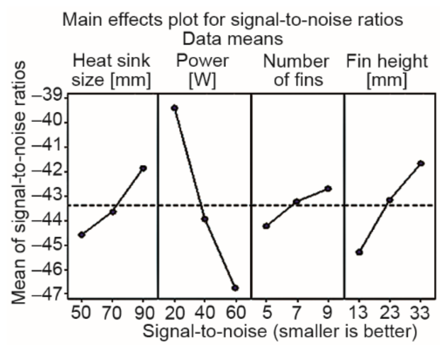

Figure 11. Main effect plot for signal-to-noise ratios

Optimization

Optimization of the heat sink is carried out through Taguchi to analyze effect of each parameter and to find optimal level for each factor as shown in fig 11. Smaller is better model for signal-to-noise ratio is considered to predict optimal conditions for the heat sink. The optimal condition for the heat sink is obtained at 90 mm heat sink size, 20 W input power, 9 number of fins, and 33 mm fins height. Combination of these level could be used to achieve maximum efficiency.

Conclusion

In this study, *L*-shape fins heat sink in investigated under natural convection with various input parameters. The energy, continuity, and momentum governing equations are discretised and solved for different input powers. The results are presented in the form of average temperature, temperature difference, ΔT, and temperature contours. The mean temperature difference is the most important parameter to evaluate performance of the heat sink at different configurations. The results revealed that increasing the clearance between the shroud and sink increases the heat transfer rate. Furthermore, ANOVA and Taguchi results disclosed that fin height is the most influential input parameter and accounts for 25.3% of total contribution. In addition, fin height of 33 mm, heat sink size of 90 mm and 9 fin numbers is found to be the optimal configuration and results in maximum heat transfer.

References

[1] Huang, C. H., Tung, P. W., Numerical and Experimental Studies on an Optimum Fin Design Problem to Determine the Deformed Wavy-Shaped Heat Sinks, *International Journal of Thermal Sciences, 151* (2020), May, 106282
[2] Duan, Z., *et al*., Analysis of Flow Characteristics and Pressure Drop for an Impinging Plate Fin Heat Sink with Elliptic Bottom Profiles, *Applied Sciences, 10* (2020), 1, 225
[3] Alfellag, M. A., *et al*., Numerical Simulation of Hydrothermal Performance of Minichannel Heat Sink Using Inclined Slotted Plate-Fins and Triangular Pins, *Applied Thermal Engineering, 164* (2020), Jan., 114509
[4] Abdelmohimen, M. A., *et al*., Improving Heat Transfer of Plate-Fin Heat Sinks Using Through Rod Configurations, *Journal of Thermal Science and Engineering Applications, 13* (2021), 1, 011003
[5] Wiriyasart, S., Naphon, P., Heat Spreading of Liquid Jet Impingement Cooling of Cold Plate Heat Sink with Different Fin Shapes, *Case Studies in Thermal Engineering, 20* (2020), Aug., 100638
[6] Freegah, B., *et al*., CFD Analysis of Heat Transfer Enhancement in Plate-Fin Heat Sinks with Fillet Profile: Investigation of New Designs, *Thermal Science and Engineering Progress, 17* (2020), June, 100458
[7] Sivapragasam, A., *et al*., Experimental Investigation on Thermal Performance of Plate Fin Heat Sinks with Nano PCM, *Thermal Science, 24* (2020), 1B, pp. 437-446
[8] Arshad, A., *et al*.,. Experimental Investigation of PCM Based Round Pin-Fin Heat Sinks for Thermal Management of Electronics: Effect of Pin-Fin Diameter, *International Journal of Heat and Mass Transfer, 117* **(**2018), Feb., pp. 861-872
[9] Pakrouh, R., *et al*., A Numerical Method for PCM-Based Pin Fin Heat Sinks Optimization, *Energy Conversion and Management, 103* **(**2015), Oct., pp. 542-552
[10] Taghilou, M., Khavasi, E., Thermal Behavior of a PCM Filled Heat Sink: The Contrast Between Ambient Heat Convection and Heat Thermal Storage, *Applied Thermal Engineering, 174* (2020), June, 115273
[11] Nair, D. V., Enhancement of Free Convection from Horizontal-Base Straight-Fin Heat Sink by Partial Shrouding, *Journal of Thermal Science and Engineering Applications, 12* (2020), 3, 031023
[12] Jones, C. D., Smith, L. F., Optimum Arrangement of Rectangular Fins on Horizontal Surfaces for Free-Convection Heat Transfer, *Journal of Heat Transfer, 92* (1970), 1, pp. 6-10
[13] Bar-Cohen, A., Fin Thickness for an Optimized Natural Convection Array of Rectangular Fins, *Journal of Heat Transfer, 101* **(**1979), 3, pp. 564-566
[14] Teertstra, P., *et al*., Analytical Forced Convection Modeling of Plate Fin Heat Sinks, *Journal of Electronics Manufacturing, 10* **(**2000), 4, pp. 253-261
[15] Baskaya, S., *et al*., Parametric Study of Natural Convection Heat Transfer from Horizontal Rectangular Fin Arrays, *International Journal of Thermal Sciences, 39* (2000), 8, pp. 797-805
[16] de Lieto Vollaro, A., *et al.*, Optimum Design of Vertical Rectangular Fin Arrays, *International journal of thermal sciences, 38* (1999), 6, pp. 525-529
[17] Mehrtash, M., Tari, I., A Correlation for Natural Convection Heat Transfer from Inclined Plate-Finned Heat Sinks, *Applied Thermal Engineering, 51* (2013), 1-2, pp. 1067-1075
[18] Shen, Q., *et al*., Orientation Effects on Natural Convection Heat Dissipation of Rectangular Fin Heat Sinks Mounted on LEDs, *International Journal of heat and mass transfer, 75* (2014), Aug., pp. 462-469
[19] Naik, S., *et al*., Natural-Convection Characteristics of a Horizontally-Based Vertical Rectangular Fin-Array in the Presence of a Shroud, *Applied Energy, 28* (1987), 4, pp. 295-319
[20] Ledezma, G., Bejan, A., Heat Sinks with Sloped Plate Fins in Natural and Forced Convection, *International Journal of heat and mass transfer, 39* (1996), 9, pp. 1773- 1783

[21] Elshafei, E., Natural Convection Heat Transfer from a Heat Sink with Hollow/Perforated Circular Pin Fins, *Proceedings*, 3rd International Conference on Thermal Issues in Emerging Technologies Theory and Applications, Cairo, Egypt, 2010, IEEE, pp. 185-19322

[22] Kim, D. K., Thermal Optimization of Plate-Fin Heat Sinks with Fins of Variable Thickness Under Natural Convection, *International Journal of Heat and Mass Transfer, 55* (2012), 4, pp. 752-761

[23] Jang, D., *et al*., The Orientation Effect for Cylindrical Heat Sinks with Application to LED light Bulbs, *International Journal of Heat and Mass Transfer, 71* (2014), Apr., pp. 496-502

[24] Costa, V. A., Lopes, A. M., Improved Radial Heat Sink for Led Lamp Cooling, *Applied Thermal Engineering, 70* (2014), 1, pp. 131-138

[25] Jang, D., *et al*., The Orientation Effect for Cylindrical Heat Sinks with Application to LED Light Bulbs, *International Journal of Heat and Mass Transfer, 71* (2014), pp. 496-502

[26] Li, B., *et al*., Enhanced Natural Convection Heat Transfer of a Chimney-Based Radial Heat Sink, *Energy conversion and management, 108* **(**2016), Jan., pp. 422-428

[27] Chamkha, A. J., *et al*., MHD Convection of an Al_2O_3-Cu/Water Hybrid Nanofluid in an Inclined Porous Cavity with Internal Heat Generation/Absorption, *Iranian Journal of Chemistry and Chemical Engineering, (IJCCE)*, On-line first, https://doi.org/10.30492/IJCCE.2021.136201.4328, 2021

[28] Kargarsharifabad, H., Experimental and Numerical Study of Natural Convection of Cu-Water Nanofluid in a Cubic Enclosure Under Constant and Alternating Magnetic Fields, *International Communications in Heat and Mass Transfer, 119* (2020), Dec., 104957

[29] Kargarsharifabad, H., Optimization of Arrangement of Conducting Fins and Insulated Obstacles Inside a Cavity: The Couple of Numerical Solutions and Genetic Algorithm Methods, *Journal of Thermal Analysis and Calorimetry, 147* (2022), 1, pp. 421-433

[30] Chamkha, A. J., *et al*., Magnetohydrodynamic Mixed Convection and Entropy Analysis of Nanofluid in Gamma-Shaped Porous Cavity, *Journal of Thermophysics and Heat Transfer, 34* (2020), 4, pp. 836-847

[31] Bahmani, A., Kargarsharifabad, H., Laminar Natural Convection of Power-Law Fluids Over a Horizontal Heated Flat Plate, *Heat Transfer-Asian Research, 48* (2019), 3, pp. 1044-1066

[32] Bahmani, A., Kargarsharifabad, H., Magnetohydrodynamic Free Convection of Non-Newtonian Power-Law Fluids Over a Uniformly Heated Horizontal Plate, *Thermal Science, 24* (2020), 2B, pp. 1323-1334

[33] Mousavi, H., *et al*., A Novel Heat Sink Design with Interrupted, Staggered and Capped Fins, *International Journal of Thermal Sciences, 127* (2018), May, pp. 312-320

[34] Haghighi, S. S., *et al*., Natural Convection Heat Transfer Enhancement in New Designs of Plate-Fin Based Heat Sinks, *International Journal of Heat Mass Transfer, 125* **(**2018), Oct., pp. 640-647

[35] Yalcin, H. G., *et al*., Numerical Analysis of Natural Convection Heat Transfer from Rectangular Shrouded Fin Arrays on a Horizontal Surface, *International Communications in Heat Mass Transfer, 35* (2008), 3, pp. 299-311

[36] Goshayeshi, H. R., *et al*., Effect of Magnetic Field on the Heat Transfer Rate of Kerosene/Fe_2O_3 Nanofluid in a Copper Oscillating Heat Pipe, *Experimental Thermal and Fluid Science, 68* (2015), Nov., pp. 663-668

[37] Holman, J. P., *Experimental Methods for Engineers,* Mc Grawand Hill, New York, USA, 2001

[38] Mostafavi, G., M. *et al.,* Effect of Fin Interruptions on Natural Convection Heat Transfer from a Rectangular Interrupted Single-Wall, *Proceedings,* International Electronic Packaging Technical Conference and Exhibition, Mani, Hi., USA, 2013

Paper submitted: June 12, 2021
Paper revised: August 12, 2021
Paper accepted: August 24, 2021